Electronic Supplementary Material (ESI) for Lab on a Chip.


# Supporting Information

## Quantitative reagent monitoring in paper-based electrochemical rapid diagnostic tests

Léonard Bezinge, Andrew J. deMello, Chih-Jen Shih and Daniel A. Richards*,

Institute for Chemical and Bioengineering, Department of Chemistry and Applied Biosciences, ETH Zürich, Vladimir-Prelog-Weg 1, 8093 Zürich, Switzerland.

* daniel.richards@chem.ethz.ch

### Content

# Experimental methods

### *Device fabrication*

The electrofluidic layer was fabricated as reported elsewhere [1,2]. In brief, cellulose paper (CF3, Cytiva) was treated with ammonium sulfamate (0.8 M, 92 g $L^{-1}$) and pyrolyzed using a 100 W $CO_2$ laser engraver (Speedy 300, Trotec) with power setting 18 (measured 4.8 W), speed 5 (measured 16 cm $s^{-1}$), 10 mm defocus using a 1.5 inch lens, 1000 laser pulses per inch and 333 lines per inch, under nitrogen atmosphere. Electrodes were rinsed with water, isopropanol and acetone, and dried overnight. The electrode layers were treated with oxygen plasma for 120 seconds at 90 W (Atto, Diener Electronic), and the channels laminated at 110°C from wax patterns deposited on a transparency (Xerox Colorqube 8570). All designs were created in Adobe Illustrator CS6. The device holders were 3D printed (SL1S, Prusa) and spring connectors were inserted and glued into the holders (5110/S-C-1.5N-AU-2.3 C connectors, PTR Hartmann). Absorbent pads (11.3 mm diameter, 3x per device, total capacity: 412 µL) were laser cut from cellulose pads (CF6, Cytiva). The nitrocellulose capture pad (8 mm diameter, AE98, Cytiva) was prepared by drop casting 5 µL of secondary antibody (goat anti-human IgG, Fc specific, Sigma, 1 mg $mL^{-1}$ in 50 mM KCl and 50 mM Tris pH 7.5) and let dry for at least 3 hours before use. A sample pad (7.5 mm diameter, CF1 or CF3, Cytiva) was placed above the capture layer in the device.

### *Nanoparticle preparation*

Nanoparticle labels were prepared by incubating 500 µL gold nanoparticle 20 nm (OD1, EM.GC20, BBI) with 20 µL borate buffer 0.5 M pH 8.3 and 0.33 µL SARS-CoV-2 nucleocapsid antigen (0.5 mg $mL^{-1}$ LA612, EastCoastBio). After 30 minutes at room temperature with 500 rpm agitation (Eppendorf ThermoMixer), 5 µL alkaline phosphatase (1.8 mg $mL^{-1}$, A2356, Sigma) was added and the mixture incubated for an additional 30 minutes. Next, the particle surface was blocked by adding 50 µL of blocking buffer (5 % bovine serum albumin, 0.05 % Tween-20 in 20 mM Tris pH 7.5, Sigma), and agitated for 30 minutes. The particles were washed twice by centrifugation (10 krpm, 4 °C, 30 minutes) and resuspended in 50 µL blocking buffer (10X AuNP).

*Nanoparticle characterization*

Absorption spectra were recorded on a plate reader (Synergy H1, BioTek) between 400 and 700 nm with a 5 nm step and 10-fold dilution of the nanoparticles in water. The enzymatic activity was monitored on the same plate reader, with a 100-fold particle dilution in 100 mM Tris pH 9.8, 20 mM $MgCl_2$ and 10 mM *p*-nitrophenyl phosphate (> 99 %, Roth). The enzymatic activity was computer by fitting a linear function to the absorption profile (405 nm), discarding the first 10 minutes (total run time of 120 min). The direct binding capacity of the particles was evaluated using SARS-CoV-2 Rapid Antigen Test (Roche Diagnostics). The test strips were scanned at 300 dpi, converted to gray scale and the test line intensity computed by integration.

*Electrochemical assay*

All electrochemical measurement were performed on a compact USB potentiostat (Sensit Smart, PalmSens). Flow monitoring was achieved by pulsed amperometry measurements with the following parameters: 0 V bias, 100 mV pulse amplitude, 1 ms pulse time and 100 ms interval, with the pulse current sampling mode. The current difference between every 10th pulse was computed and a moving average with span 10 applied to the data. The threshold was computed by taking the average absolute current differences + 10 standard deviations, applied to measurements recording during 100 s after injection of 100 µL of 20 mM Tris·HCl pH 7.5. Buffer solutions containing Tris·HCl, Tween-20 (>97%, Sigma) and bovine serum albumin (BSA, > 98%, Sigma) were prepared to study the flow responses.

For testing of the serum samples, a running buffer (5 wt% BSA, 0.05 vol% Tween-20 in 20 mM Tris·HCl pH 7.5) and rinsing buffer (0.1% Tween-20, 20 mM Tris·HCl pH 7.5) were prepared. Serum samples were purchased from commercial suppliers: normal human serum (Catalog # 31876, Invitrogen) and reference human serum with antibodies against SARS-CoV-2 (EURM-17, Sigma) were used as positive and negative controls, respectively. The testing procedure consisted of the sequential injection of 100 µL sample (10 µL serum diluted 10-fold in running buffer), 100 µL gold nanoparticle in running buffer, 150 µL of rinsing buffer and 25 µL of substrate solution (10 mM *p*-aminophenyl phosphate in 100 mM

Tris·HCl pH 9.8 and 20 mM $MgCl_2$). After 15 min, the signal was quantified by square wave voltammetry with the following parameters: 5 s equilibration, start potential -0.2 V, end potential 0.25 V, step 5 mV, pulse amplitude 25 mV and frequency 2.5 Hz.

For the combined flow tracking and electrochemical serology assay, a custom python script was developed to control the Sensit potentiostat via the MethodSCRIPT v1.3 protocol (PalmSens).

### *Statistical analysis*

Unless mentioned otherwise, measurements are performed in triplicate (n=3) and the median value shown. The error bars correspond to the associated 25–75\% percentile range (interquartile range, IQR). Significance and p-values are computed using a two-sample Kolmogorov-Smirnov test. In the case of fitted curves, the confidence interval is shown as a shaded area for one standard deviation in each direction. MATLAB (R2022b) was used for all data processing and statistical analysis.

## Supplementary Figures

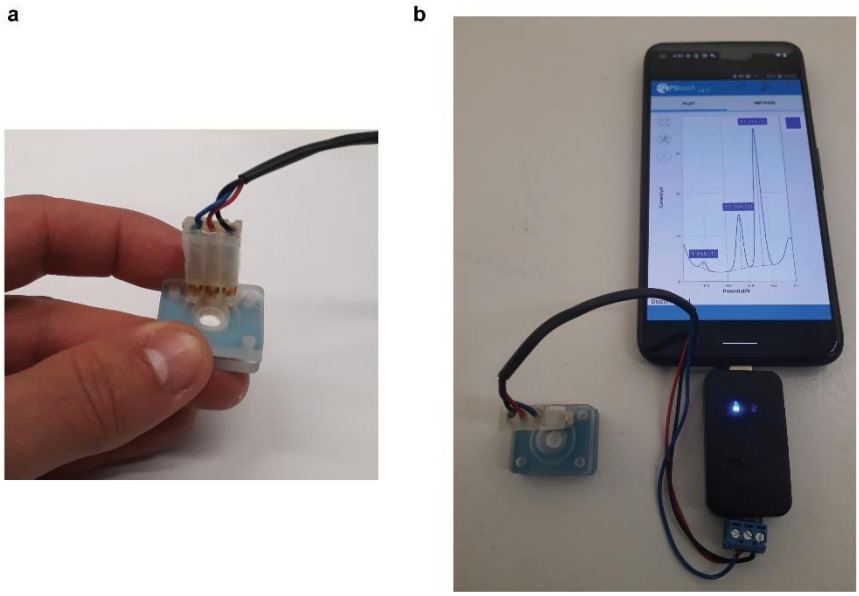


**Figure S1:** Pictures of (a) the assembled electrochemical vertical flow device and (b) the measurement setup, including the compact USB potentiostat, in this case connected to a smartphone.

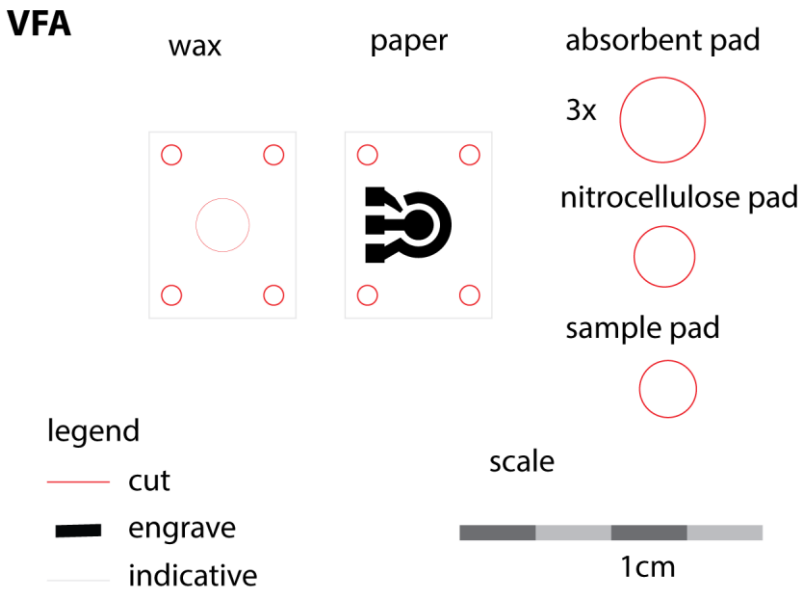


**Figure S2:** Fabrication design for the vertical flow device.

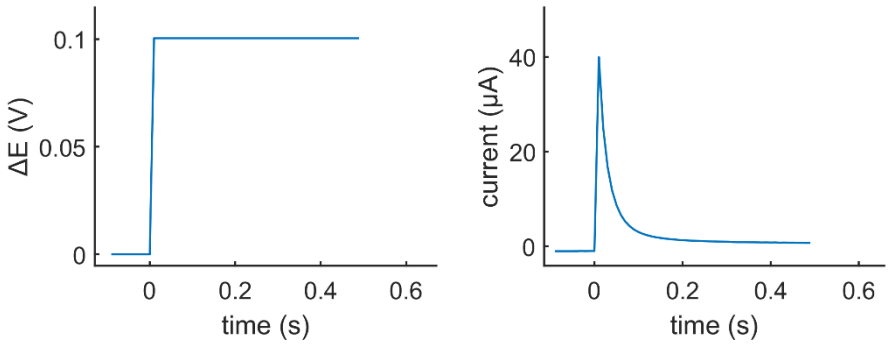


**Figure S3:** Current response following a 0.1V potential step in 20 mM Tris·HCl buffer. Using the approximate method from Bard *et al.*, we estimate the double-layer capacitance at about 12 mF ($i_{peak} = \Delta E/R_s$, and $\tau_{37\%} = R_s C_d$, where $i_{peak}$ is the peak current, $R_s$ the solution resistance and $\tau_{37\%}$ the decay time to reach 37% of the max current value) [3].

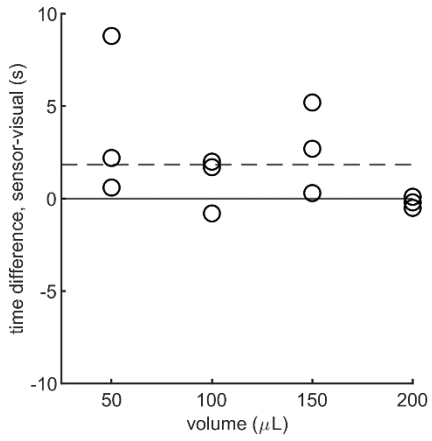


**Figure S4:** Bland-Altman plot for the difference in flow times recorded by our method compared to visual inspection. Recorded flow times were significantly longer ($p < 0.05$), with an average of +1.8 s (dashed line).

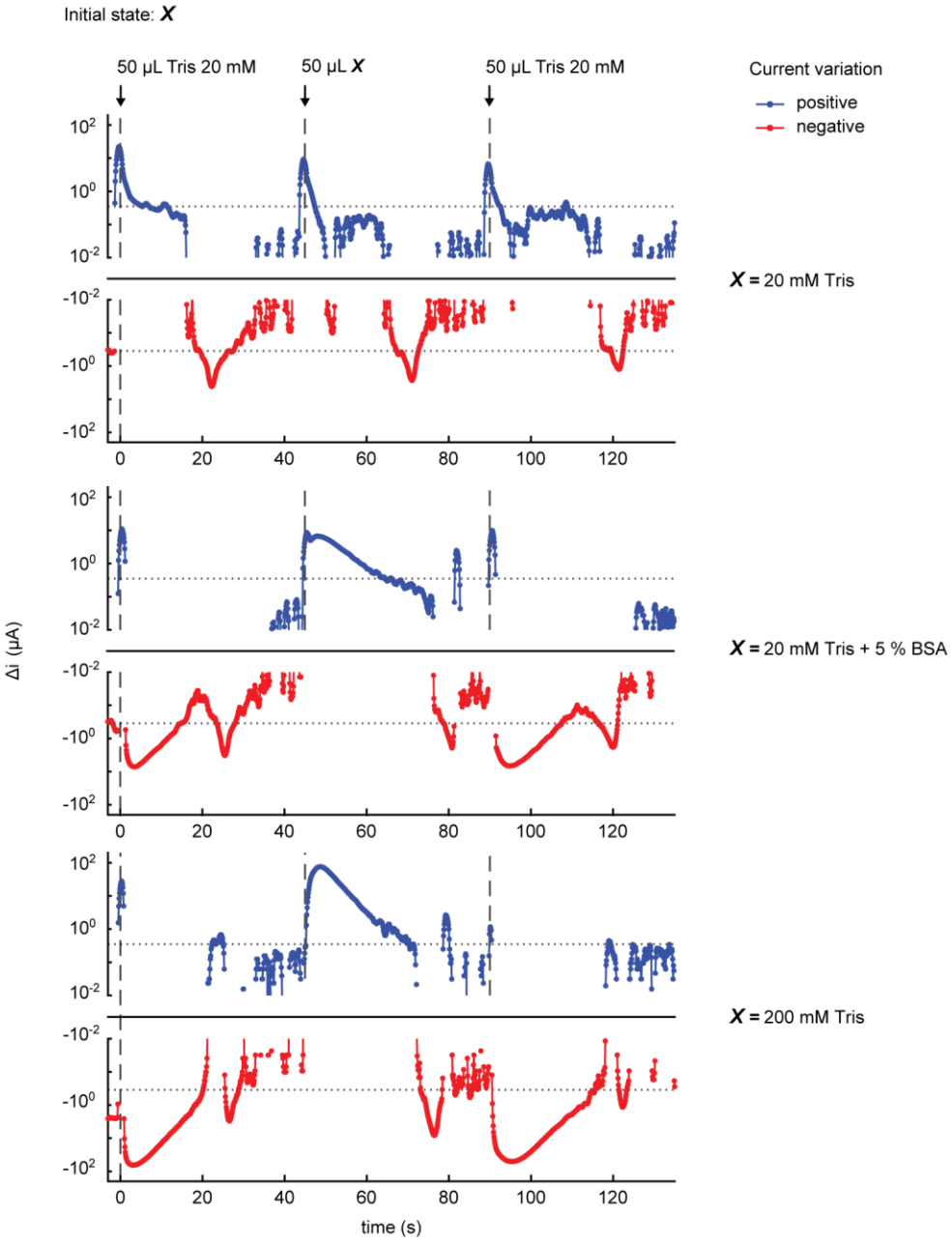


**Figure S5:** Sequential addition of buffer solutions (50 µL) with alternating composition. The current variations is shown in log-scale, with the positive and negative displayed in blue and red, respectively. All buffers also contain 0.05 vol-% Tween-20. Variations were positive for increasing flow rates or ionic strength (compared to the previous injection), whereas decelerating flow rates, lower ionic strength or rinsing albumin off the electrodes resulted in negative variations.

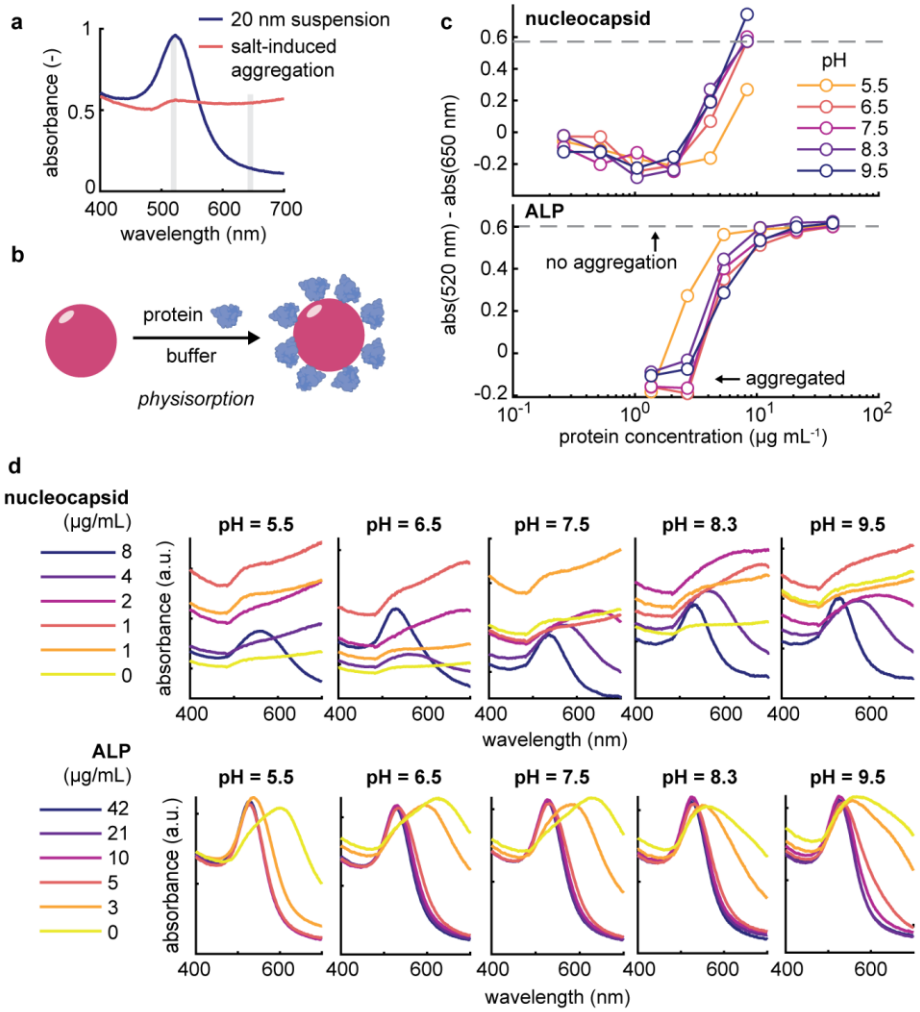


**Figure S6:** (a) Absorption spectra of the 20 nm gold nanoparticle suspension before and after salt addition. The difference between the absorption at 520 nm and 650 nm serves as an indicator of aggregation [4]. (b) Schematic of the single protein physisorption process. (c) Degree of aggregation for gold nanoparticles incubated with nucleocapsid or alkaline phosphatase (ALP) at different concentrations and pH, including the absorption spectra in the visible range (d) [5].

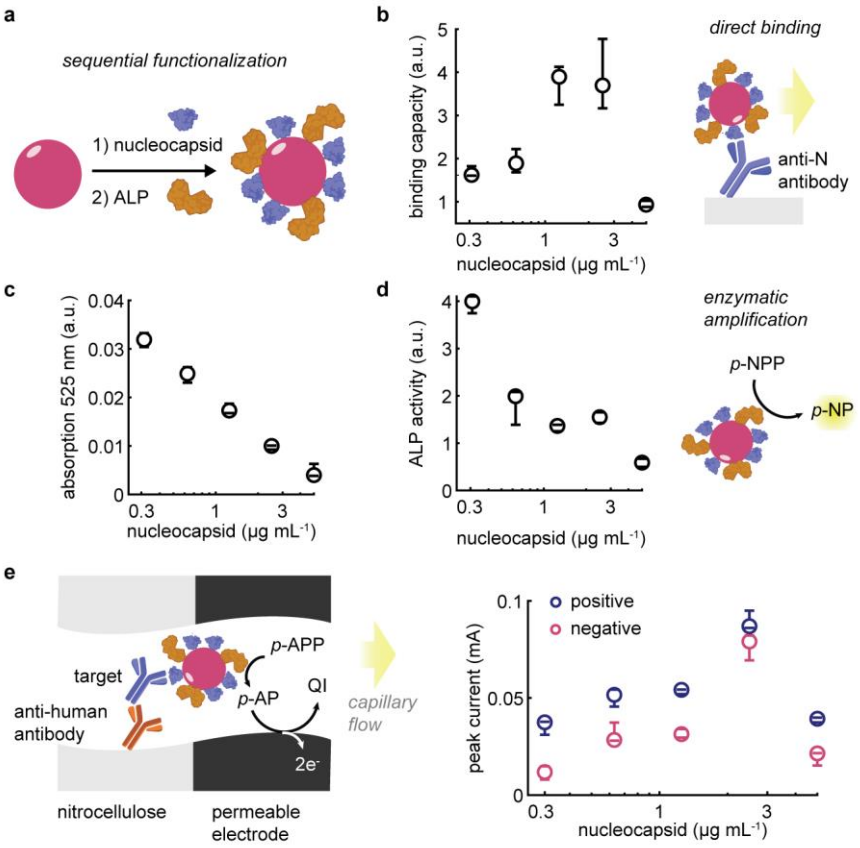


**Figure S7:** (a) Functionalization of gold nanoparticles in a sequential two-step process. (b) The binding capacity of the nanoparticles was derived colorimetrically from the test line intensity using a commercial rapid test with anti-nucleocapsid capture line. (c) Intensity of the absorption peak at 525 nm with increasing nucleocapsid coverage. (d) Enzymatic activity evaluated using the colorimetric substrate \textit{p}-nitrophenyl phosphate. (e) Capillary-driven electrochemical test using a nitrocellulose capture layer and paper-embedded graphenic electrodes. The signals, derived from the peak height of square wave voltammogram, are displayed for anti-SARS-CoV-2 IgG positive and negative serum (n=3). *p*-NPP: *p*-nitrophenyl phosphate, *p*-NP: *p*-nitrophenol, *p*-APP: *p*-aminophenyl phosphate, *p*-AP: *p*-aminophenol, QI: 4-quinoneimine.

## References


(1) Bezinge, L.; Lesinski, J. M.; Suea-Ngam, A.; Richards, D. A.; deMello, A. J.; Shih, C. Paper-Based Laser-Pyrolyzed Electrofluidics: An Electrochemical Platform for Capillary-Driven Diagnostic Bioassays. *Adv. Mater.* **2023**, 2302893. https://doi.org/10.1002/adma.202302893.

(2) Bezinge, L.; Tappauf, N.; Richards, D. A.; Shih, C.-J.; deMello, A. J. Rapid Electrochemical Flow Analysis of Urinary Creatinine on Paper: Unleashing the Potential of Two-Electrode Detection. *ACS Sens.* **2023**, *8* (10), 3964–3972. https://doi.org/10.1021/acssensors.3c01640.

(3) Bard, A. J.; Faulkner, L. R.; White, H. S. *Electrochemical Methods: Fundamentals and Applications*; Wiley, 2022.

(4) Parolo, C.; Sena-Torralba, A.; Bergua, J. F.; Calucho, E.; Fuentes-Chust, C.; Hu, L.; Rivas, L.; Álvarez-Diduk, R.; Nguyen, E. P.; Cinti, S.; Quesada-González, D.; Merkoçi, A. Tutorial: Design and Fabrication of Nanoparticle-Based Lateral-Flow Immunoassays. *Nat. Protoc.* **2020**, *15* (12), 3788–3816. https://doi.org/10.1038/s41596-020-0357-x.

(5) Sotnikov, D. V.; Berlina, A. N.; Ivanov, V. S.; Zherdev, A. V.; Dzantiev, B. B. Adsorption of Proteins on Gold Nanoparticles: One or More Layers? *Colloids Surf. B Biointerfaces* **2019**, *173*, 557–563. https://doi.org/10.1016/j.colsurfb.2018.10.025.